Journal of GeoEngineering, Vol. 17, No. 2, pp. 103-112, June 2022
http://dx.doi.org/10.6310/jog.202206_17(2).4

POLYURETHANE ORGANIC POLYMER AS AN ECO-FRIENDLY SOLUTION FOR IMPROVEMENT OF SHEAR STRENGTH OF SAND-FLY ASH MIXTURES

Hamou Azaiez [1], Abdellah Cherif Taiba [2*], Youcef Mahmoudi [2], and Mostefa Belkhatir [3]

ABSTRACT

Results of an experimental study on the use of polyurethane organic polymer to improve the compressive strength of a mixture of sand-fly ash considering the influence of particle morphology characteristics is discussed in this paper. In this context, a set of unconfined compression tests were performed on reconstituted samples at room temperature approximating 25°C. The samples were mixed with four fly ash contents, 0%, 5%, 10%, and 15%, and four polyurethane organic polymer contents ranging from 2% to 8%. The obtained outcome indicates that the polyurethane organic polymer (POP) has a remarkable influence on the unconfined compressive strength (UCS) of the sand-fly ash mixtures. New proposed parameters suggested based on a combination of particle shape properties of the mixture have been introduced in this paper to evaluate their effects on the UCS of the studied materials. Moreover, the analysis of the generated data confirms the existence of simple correlations relating particle shape characteristics and granulometric properties to the unconfined compressive strength of the POP-enhanced sand-fly ash mixtures under consideration. In addition, the combined overall regularity parameter appears as a reliable parameter in predicting the unconfined compressive strength of the tested materials compared to the other particle morphology properties. Therefore, the present investigation clearly outlines the relevance of the particle morphology characteristics and their effects on the UCS of the tested materials and consequently, contributes adequately in the prediction of the UCS of the POP-improved sand-fly ash mixtures based on particle shape and size properties.

Key words: Polyurethane organic polymer, sand-fly ash mixtures, particle characteristics, overall regularity.

1. INTRODUCTION

Particle morphology properties (in terms of shape and size) of soils are commonly considered as relevant parameters that influence and consequently, control the mechanical behaviour of granular materials. Therefore, their proper evaluation conducts to a better comprehension of soil shearing response (Santamarina and Cho 2004; Cho *et al.* 2006; Guo *et al.* 2007; Tsomokos *et al.* 2010; Yang *et al.* 2015; Altuhafi *et al.* 2016; Cherif Taiba *et al.* 2018; Xiao *et al.* 2019; Doumi *et al.* 2020; Mahmoudi *et al.* 2020b; Cherif Taiba *et al.* 2022; Mahmoudi *et al.* 2022). Wadell (1932) was the first researcher who evaluated the particle shape in terms of sphericity of granular soils where he defined it as the ratio of the curvature of the corners and edges to that of the overall particle. However, published literature has commonly reported the evaluation of the overall regularity of soils. Moreover, Cho *et al.* (2006) subdivided the particle shape properties into six different categories of angularity: very angular, angular, sub-angular, sub-rounded, rounded and well rounded. In the case of particle sphericity, they adopted two categories: low sphericity and high sphericity (Fig. 1). Therefore, many researches have focused on the evaluation of the relationship between particle shape properties and the shearing response of natural and crushed soils. Wei and Yang (2014) reported that the vulnerability of sand-silt mixtures to liquefaction may be influenced by the sand and silt grain shapes. Khayat *et al.* (2014) found that the particle shape may affect the anisotropic response of silty sand soils. They confirmed that the higher roundness and sphericity of sand exhibited contractive responses under hollow cylinder torsion shear tests. Yang and Wei (2015) observed that the angular shape of the coarse sand mixed with angular silt had a higher resistance compared to that of the rounded sand mixed with angular fines grains. (Cherif Taiba *et al.* 2018, 2021) found that the grain shape of sand had a noticeable impact on the behavior of silty sand soils for the lower fines' contents ($F_c \leq 30\%$). Xiao *et al.* (2019) confirmed that the particle shape impacted significantly the stress-dilatancy response of the tested medium dense sands; where, they found that the medium dense sand exhibited typical strain-softening and dilative responses for the particle shape parameter (overall regularity) from 0.844 to 0.971.

On the other hand, it is well known that particle characteristics play an influential role on the macroscopic mechanical response of natural granular soils (Varadarajan *et al.* 2003; Frossard *et al.* 2012; Dai *et al.* 2016; Zhang *et al.* 2016; Zhou *et al.* 2016; Cherif Taiba *et al.* 2019b; Xiao *et al.* 2019, Doumi *et al.* 2021 and Mahmoudi *et al.* 2021). Kokusho *et al.* (2004) observed that the undrained strength depends on the particle size in terms of the coefficient of uniformity for larger strain from 20% to 25%, mentioning that the increase of the coefficient of uniformity (C_u) in-

Manuscript received November 25, 2021; revised March 14, 2022; accepted April 26, 2022.
[1] PhD. candidate, Laboratory of Structures, Geotechnics and Risks, University of Chlef (Algeria).
[2*] Associate Professor (corresponding author), Laboratory of Material Sciences & Environment, University of Chlef (Algeria) (e-mail: a.cheriftaiba@univ-chlef.dz).
[3] Professor, Alexander von Humboldt Foundation Researcher (Germany).

duced an increase of the undrained shear strength. Janalizadeh *et al.* (2013) showed that the cyclic resistance of the soil could be expressed in terms of the granulometric properties (*i.e.,* D_{10}, D_{30}, or D_{60}) rather than the coefficient of uniformity (C_u) or the coefficient of curvature (C_c) of the tested soils. Cherif Taiba *et al.* (2019a) reported that the particle size influenced in a significant manner the undrained shear strength of the sand-silt mixtures. Monkul *et al.* (2016) indicated that the particle size had a pivotal impact on the static liquefaction potential of clean and silty sands.

However, the improvement as well as the treatment of granular soils with additive materials such as pozzolan, lime and fly ash (Lo and Wardani 2002; Saeid *et al.* 2012; Azaiez *et al.* 2021b), or eco-friendly solutions like polymers (xanthan gum, chitosan gum, polyurethane organic polymer) (Su and Zhang 2011; Latifi *et al.* 2016; Dehghan *et al.* 2019; Ghasemzadeh *et al.* 2021) were commonly practiced worldwide to achieve higher mechanical performance of these soils. Jais *et al.* (2017) showed that the injection of the organic polymer into the road subgrade layers exhibited a noticeable increase of the soil's characteristics in terms of stiffness and bearing capacity. Liu *et al.* (2018) performed a series of unconfined compressive strength tests on sandy soils treated with polymer contents (PSS = 10%, 20%, 30%, 40%, and 50%). They found that the unconfined compressive strength properties of sand were remarkably improved by polymer soil stabilizer (PSS). Xiao *et al.* (2018) indicated that a gravelly soil improved by polyurethane organic polymer could be considered as a reliable material in the transportation infrastructure applications.

Meanwhile, these previous researches have focused on the enhancement of shearing behaviour of the granular soils by using these newest materials and solutions without emphasizing and taking into account the influence of soil properties (*i.e.,* particle size and shape). Moreover, in the previous research studies cited above, no attempt was made to predict the influence of the particle characteristics (shape and size) on the shearing response of the sand-fly ash mixtures improved by the polyurethane organic polymer (POP). To achieve this goal, an experimental investigation has been carried out on Chlef sand mixed with fly ash (FA = 0%, 5%, 10%, and 15%) and polyurethane organic polymer content (W_p = 2%, 4%, 6%, and 8%) to develop physical correlations relating the unconfined compressive strength (UCS) to the particle morphology characteristics, *i.e.,* effective particle diameter D_{10}, mean particle diameter D_{50}, coefficient of uniformity C_u, combined angularity A_{com}, combined sphericity S_{com}, combined aspect ratio AR_{com}, combined convexity Cx_{com}, and combined overall regularity OR_{com}.

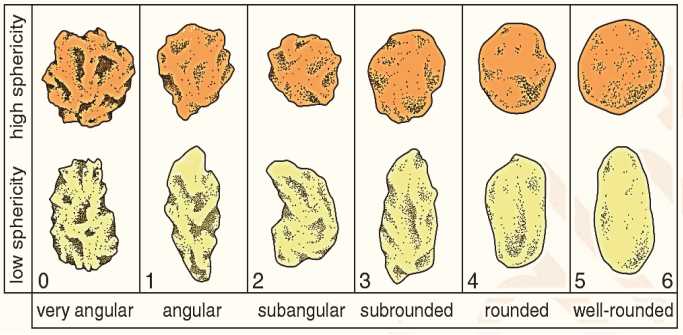

Fig. 1 Categories of particle shape properties illustrated by Cho *et al.* (2006)

2. CHARACTERISTICS OF SAND-FLY ASH MIXTURES AND TESTING PROTOCOLS

2.1 Investigated Materials

The sand was collected from liquefied soil deposition areas along the banks of Chlef River (north of Algeria) (Mahmoudi *et al.* 2020a and Azaiez *et al.* 2021a). The sand was sieved, washed and oven dried before testing and then discarded. It has a maximum grain size of D_{max} = 2.00 mm with rounded shape according to Cherif Taiba *et al.* (2018) and a specific gravity of G_s = 2.64, mean particle diameter D_{50} = 0.430 mm, coefficient of uniformity C_u = 3.441, and coefficient of curvature C_c = 1.126. The investigated sandy soil is classified as poorly graded sand (SP) according to the Unified Soil Classification System (USCS), as shown in Fig. 2(a). The fly ash material used, as shown in Fig. 2(b), is in spherical shape according to Kermatikerman *et al.* (2018) and is provided by the cement plant of Chlef city. Its chemical composition is shown in Table 1. The index properties of the sand-fly ash mixtures are shown in Table 2. The particle size distribution curves of the used sand mixed with different fly ash contents are illustrated in Fig. 3. In addition, the polyurethane organic polymer, as shown in Fig. 2(c), is commonly used in several industrial applications. Recently, it is considered as a reliable material by researchers to improve the geotechnical engineering properties of granular soils (Xiao *et al.* 2018). The polyurethane organic polymer (POP) is prepared in an exothermic chemical reaction

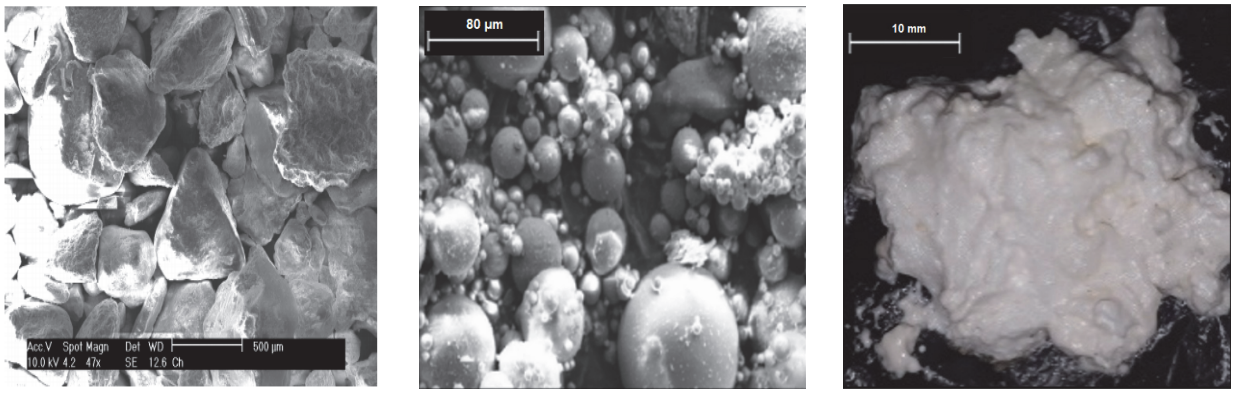

(a) Sand (b) Fly ash (c) Polyurethane organic polymer

Fig. 2 Test materials

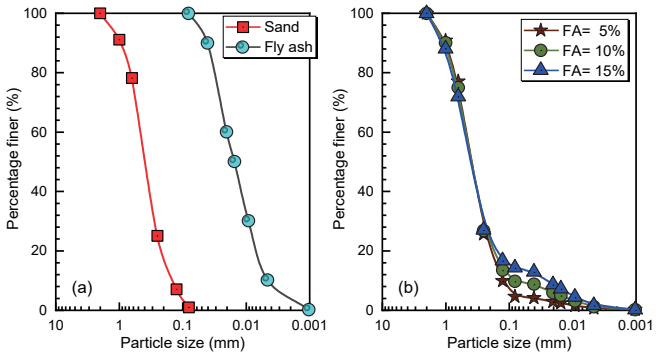

(a) Sand and fly ash (b) Sand-fly ash mixtures

Fig. 3 Particle size distribution curves

Table 1 Chemical components of fly ash

Constitutions	Percentages (%)
Silica (SiO_2)	22.3
Alumina (Al_2O_3)	5.13
Iron Oxide (Fe_2O_3)	3.78
Calcium Oxide (CaO)	66.67
Magnesium Oxide (MgO)	0.47
Titanium Oxide (TiO_2)	0.5
Loss on Ignition (LOI)	0.5 ~ 3

between diisocyanate groups and polyol monomers with two or more hydroxyl-groups. Its popularity stems partially for its low thermal conductivity, workability, and lightweight characteristics (Xiao *et al.* 2018). When mixed with dry sands, the polyurethane organic polymer can expand into the void gaps to partially or fully encapsulate nearby soil particles and conduct to the adhesive bond along the soil particle contacts (Xiao *et al.* 2018).

2.2 Evaluation of Particle Shape of the Tested Materials

In the published literature, many researchers proposed different methods for the determination, description and quantification of particle shape characteristics (Cho *et al.* 2006; Cherif Taiba *et al.* 2018). Moreover, Yang and Luo (2015) suggested four definitions of the particle shape properties named as: sphericity ($S = P_{eq}/P_r$), aspect ratio ($AR = D^F_{min}/D^F_{max}$), convexity ($Cx = A/(A+B)$) and overall regularity ($OR = S + AR + Cx)/3$, where, P_{eq}: Perimeter equivalent of sphere, P_r: Perimeter of the particle, D^F_{min}: Minimum Feret diameter, D^F_{max}: Maximum Feret diameter, A: Area of particle, $A+B$: Area of particle's convex hull. These characteristics are illustrated in Fig. 4. Moreover, the evaluation of the particle shape properties of the tested materials were usually measured using a software through a digital microscope device named (SEM: Scanning Electron Microscope). In addition, new correlations were introduced in this paper based on particle shape properties of sand ($A_{hs} = 0.453$, $S_{hs} = 0.753$, $AR_{hs} = 0.816$, $Cx_{hs} = 0.908$, $OR_{hs} = 0.826$) and those of fly ash ($A_f = 1$, $S_f = 1$, $AR_f = 1$, $Cx_f = 1$, $OR_f = 1$) (Table 3) for the purpose of relating the unconfined compressive strength with the particle shape properties of the tested materials according to the following equations:

$$A_{com} = A_{hs} \times (1 - FA) + R_f \times FA \quad (1)$$

$$S_{com} = S_{hs} \times (1 - FA) + S_f \times FA \quad (2)$$

$$AR_{com} = AR_{hs} \times (1 - FA) + AR_f \times FA \quad (3)$$

$$Cx_{com} = Cx_{hs} \times (1 - FA) + Cx_f \times FA \quad (4)$$

$$OR_{com} = OR_{hs} \times (1 - FA) + OR_f \times FA \quad (5)$$

Table 2 Index properties of the tested sand-fly ash mixtures

Property		Sand	FA = 5%	FA = 10%	FA = 15%	Fly ash
Maximum grain size (mm)	D_{max}	2.00	2.00	2.00	2.00	0.08
Specific gravity	G_s	2.64	2.662	2.684	2.71	3.08
Effective particle diameter (mm)	D_{10}	0.145	0.128	0.085	0.027	0.0045
Mean particle diameter (mm)	D_{50}	0.43	0.427	0.425	0.419	0.015
Coefficient of uniformity	C_u	3.441	3.95	6.012	19.511	4.444
Coefficient of curvature	C_c	1.126	1.247	1.747	5.311	0.9
Unified Soil Classification System	USCS	SP	SP	SP	SP	Class C
Grain shape	–	Rounded	Rounded	Rounded	Rounded	Spherical

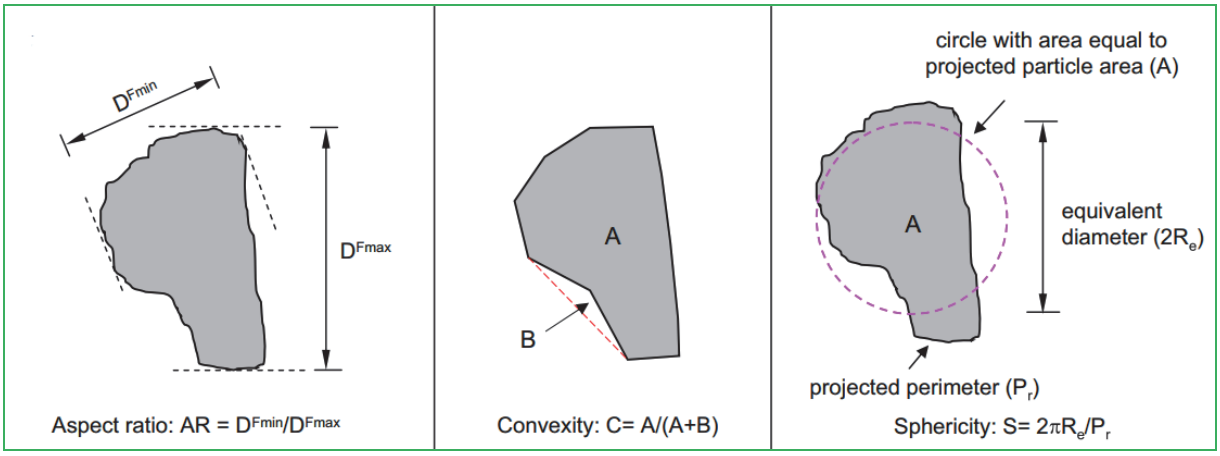

Fig. 4 Evaluation of particle shape properties (Yang and Luo 2015)

Table 3 Particle shape properties of the examined materials

Material	*A*	*S*	*AR*	*Cx*	*OR*
Host sand (*Hs*)	0.453	0.753	0.816	0.908	0.826
Fly ash (*FA*)	1	1	1	1	1

2.3 Sample Reconstitution and Unconfined Compression Tests

In this experimental investigation, the tested sand was mixed with fly ash fractions from FA = 0% to 15% and polyurethane organic polymer proportions W_p = 2%, 4%, 6%, and 8%. First, the required amounts of fly ash (*FA*= 0%, 5%, 10%, and 15%) were added to the dry soils and mixed until a homogeneous mixture was obtained. Thus, the polyurethane organic polymer is reconstituted in an exothermic chemical reaction between diisocyanate groups and polyol monomers with two or more hydroxyl groups. Thereafter, the amounts of POP were chosen as 2%, 4%, 6%, and 8% of the total weight of the mixture. These amounts of POP were mixed with the soil samples. Since the soils tended to clump, considerable attention and time was spent in order to obtain a homogeneous distribution of the mixture. The under-compaction method proposed by Ladd (1978) was used to prepare the samples. The mixture was subdivided into three layers and compacted to approximately a target density of 90%. The weight of the samples was calculated as:

$$W_{sample} = (V_{mold} \times G_s)/[(1 + e_{max} - D_r \times (e_{max} - e_{min})] \quad (6)$$

The cylindrical samples with a diameter of 40 mm and a height of 80 mm were used for all unconfined compression tests and were prepared at a room temperature of approximately 25°C. Each mixture was carefully placed into the PVC mold and compacted to a degree slightly greater than that of the underlying layer to obtain a more uniform density (D_r = 90%) throughout the samples (Polito and Martin 2001; Xiao *et al.* 2019), then tested after 24 hours of curing (Fig. 5). Furthermore, a set of unconfined compression tests were carried out in accordance with ASTM D2166 (2016) to measure the unconfined compressive strength (UCS) "q_u" of the tested sand-fly ash mixtures enhanced with polyurethane organic polymer under consideration (Table 4). A loading rate of 1mm/min was adopted. During the loading, the samples are placed in sealed bags to avoid the scattering of fragments that may spall from the samples during loading (Fig. 6).

Table 4 The samples and conditions of the examined materials

Test	FA (%)	POP (%)	D_r (%)	q_u (MPa)
Sample T01	0	2	90	0.61
Sample T02		4		1.41
Sample T03		6		1.56
Sample T04		8		2.84
Sample T05	5	2		1.2
Sample T06		4		1.95
Sample T07		6		2.47
Sample T08		8		5.14
Sample T09	10	2		0.42
Sample T10		4		1.84
Sample T11		6		3.69
Sample T12		8		6.48
Sample T13	15	2		0.4
Sample T14		4		1.67
Sample T15		6		3.73
Sample T16		8		6.76

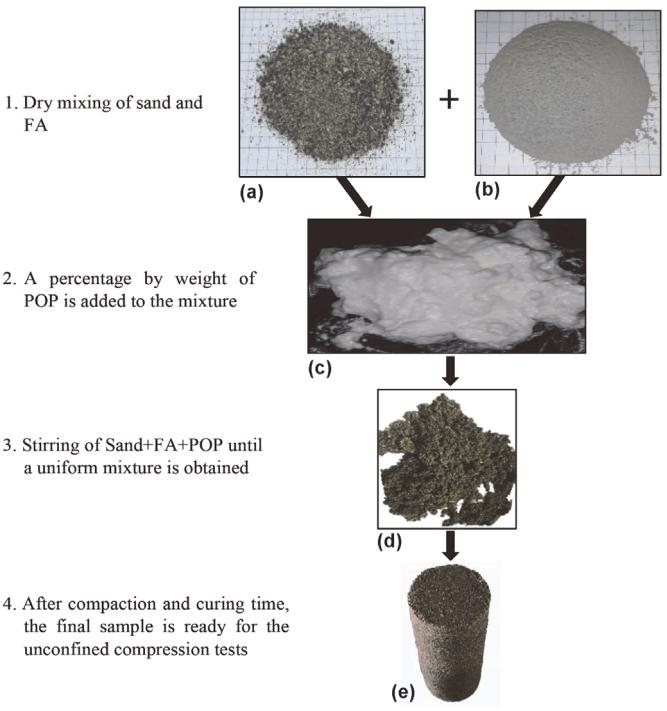

Fig. 5 Sample preparation flow chart: (a) Chlef sand; (b) fly ash; (c) POP; (d) sand-fly ash-POP mixtures; and (e) prepared sample

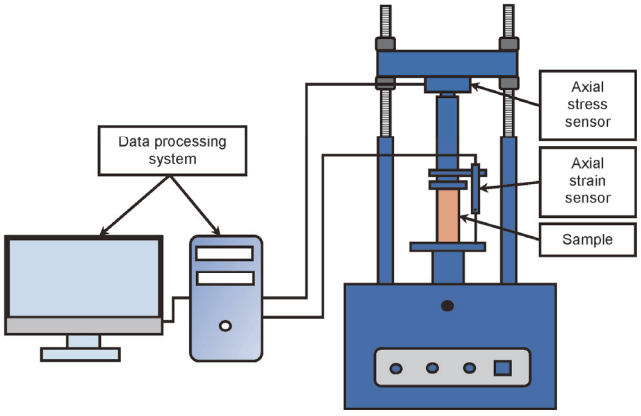

Fig. 6 Unconfined compressive test apparatus

3. UNCONFINED COMPRESSIVE STRENGTH RESULTS

Figure 7 illustrates typical stress-strain curves of the Chlef sand mixed with fly ash percentages ranging from FA = 0% to 15% stabilized with polyurethane organic polymer proportions (W_p) varying from 2% to 8%. It is clear from this figure that the addition of the polyurethane organic polymer from W_p = 2% to 8% considerably increases the axial stress at the peak state (q_u) of the tested samples. The q_u increases by 4.7 times, 4.3 times, 15.3 times, and 16.7 times for the fly ash fractions (FA = 0%, 5%, 10%, and 15%) for the sand-fly ash mixtures, respectively. Moreover, the ductility of the tested mixtures increases with increasing the polyurethane organic polymer content (W_p), *e.g.,* the axial strain at the peak state (ε_u) varies from 1.62% to 3.19%,

from 1.33% to 3.17%, from 0.83% to 1.66%, and from 0.75% to 2.11% for the used percentages of FA = 0%, 5%, 10%, and 15%, respectively. As it can be noticed the tested mixtures exhibited higher values of the unconfined compressive strength (UCS) for the highest values of the polyurethane organic polymer (W_p = 8%) and fly ash (FA = 15%) contents. This tendency clearly shows that POP enhances the UCS behavior of the sand-fly ash mixtures as well as the ductility of the mixtures under consideration. The obtained tendency can be attributed to the chemical potential of the polyurethane organic polymer inducing a strong bonding between sand and fly ash particles. Meanwhile, the pores between the sand and fly ash particles were also sufficiently filled leading to harder and more compact structures of the material (Figs. 8 and 9). In addition, Fig. 10 illustrates the mechanism of stabilization of the tested soil using the polyurethane organic polymer and fly ash material. In the absence of spherical fly ash particles, the polyurethane organic polymer (POP) tends to form lumps within the pores of sand (Fig 10(a)). With the addition of fly ash material, the POP favorites the formulation of an improved flow behavior of mixtures resulting in higher stabilization effects, and consequently conducting to higher resistance of the tested binary assemblies (Fig. 10(b)).

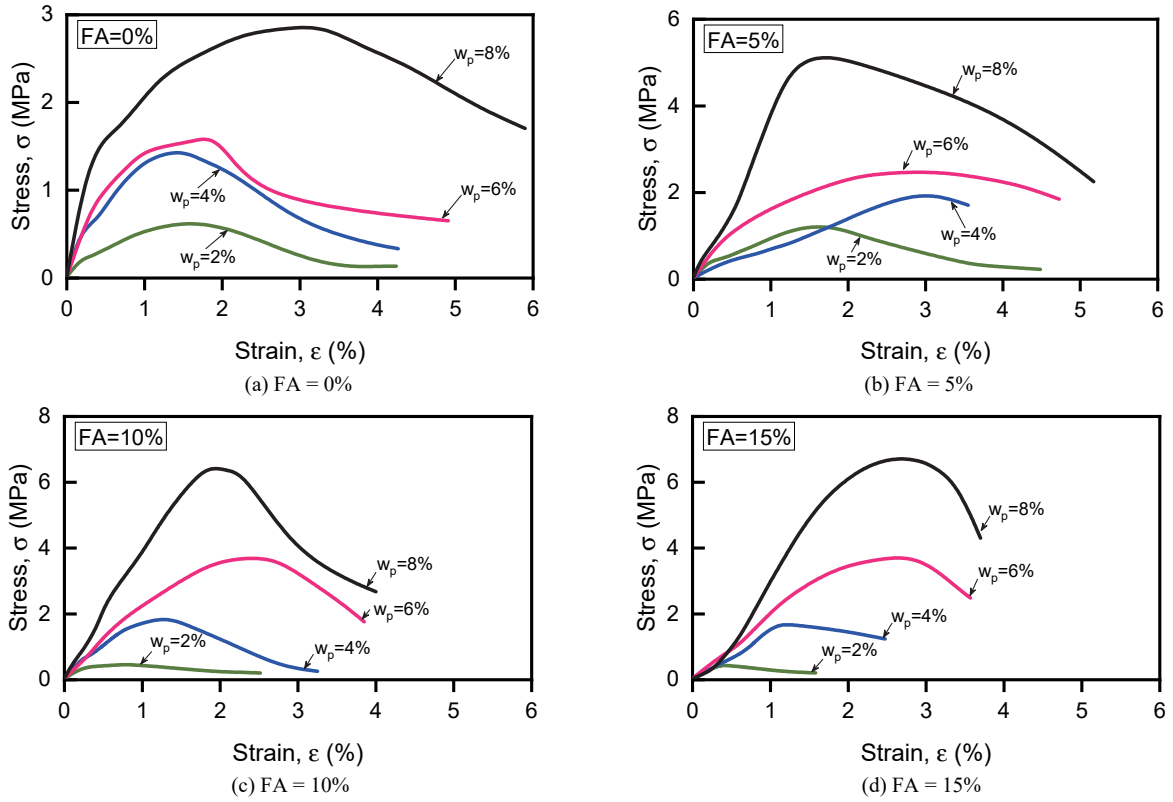

(a) FA = 0% (b) FA = 5%

(c) FA = 10% (d) FA = 15%

Fig. 7 Axial stress *vs.* axial strain curves of the sand-fly ash enhanced with the polyurethane organic polymer (2% ~ 8%)

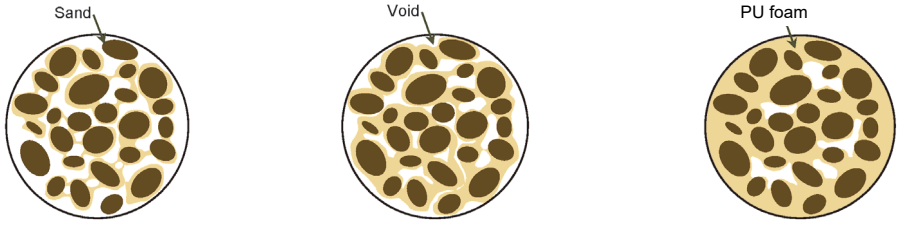

(a) W_p = 2% with FA = 0% (b) W_p = 4% with FA = 0% (c) W_p = 8% with FA = 0%

Fig. 8 Schematic diagram showing the polyurethane organic polymer concentrations without fly ash

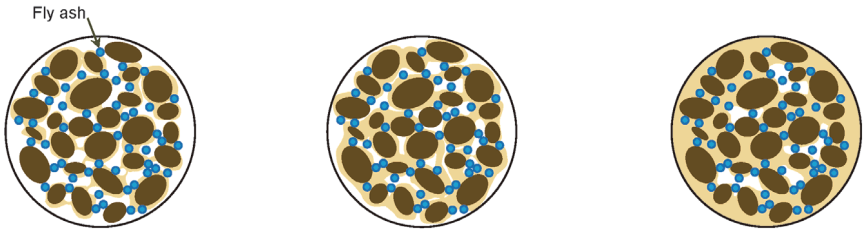

(a) W_p = 2% with FA = 15% (b) W_p = 4% with FA = 15% (c) W_p = 8% with FA = 15%

Fig. 9 Schematic diagram showing the polyurethane organic polymer concentrations with the addition of fly ash

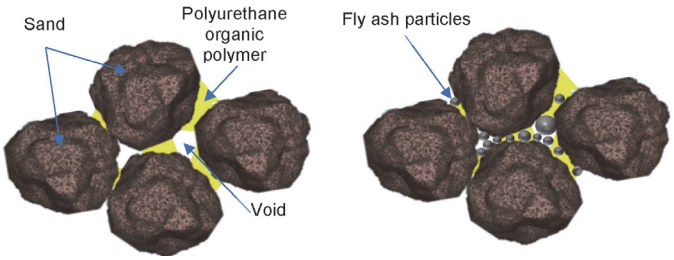

Fig. 10 Schematic representation of the mechanism of stabilization by polyurethane organic polymer and fly ash material

4. CORRELATION BETWEEN PARTICLE SHAPE PROPERTIES AND UCS OF THE TESTED MATERIALS

Figure 11 presents the variation of peak stress (q_u) with the polyurethane organic polymer content (W_p = 2%, 4%, 6%, and 8%) and the combined particle shape properties of sand and fly ash using equations 1 to 5, the combined properties are named as (combined angularity "A_{com}", combined sphericity "S_{com}", combined aspect ratio "AR_{com}", combined convexity "Cx_{com}" and combined overall regularity "OR_{com}"). It seems from this figure that the increase of POP increases the unconfined compressive strength of the mixtures under study. Moreover, as it can be seen from the 3D plot, the particle shape characteristics have a remarkable effect on the unconfined compressive strength of different sand-fly ash mixture samples. The overall soil trend indicates that the influence of the particle shape properties is clearly observed for the lower polyurethane organic polymer content (W_p = 2%) and become very pronounced for the higher polyurethane organic polymer (W_p = 8%). In addition, Fig. 11 indicates that the unconfined compressive strength increases with the increase of the combined particle shape characteristics (A_{com}, S_{com}, AR_{com}, Cx_{com}, and OR_{com}) of the tested materials. Indeed, the higher particle shape characteristics (A_{com} = 0.535, S_{com} = 0.790, AR_{com} = 0.844, Cx_{com} = 0.922, and OR_{com} = 0.852) exhibit higher values of the unconfined compressive strength (UCS = 6.76 MPa), especially, for the polyurethane organic polymer (W_p = 8%) under consideration. The observed unconfined compressive strength response is a result of the fact that the increase of the combined particle shape properties of sand and fly ash with addition of the POP induces a higher resistance of the different binary assemblies leading to hardening soil sample structures. On the other hand, Fig. 11(e) presents the variation of the UCS versus W_p and overall regularity of the sand-fly ash mixtures. From this figure, it is clear that there is a good correlation between the overall regularity and the unconfined compressive strength of the POP-improved sand-fly ash assemblies under study with a coefficient of determination (R^2 = 0.96). The correlation between these three parameters can be expressed by the following Eq. (7):

$$\begin{aligned} UCS = &-3513.33 \times (OR_{com})^2 + 0.087 \times (W_p)^2 + 28.94 \\ &\times (OR_{com}) \times (W_p) + 5812.12 \times (OR_{com}) - 24.39 \\ &\times (W_p) - 2400 \end{aligned} \quad (7)$$

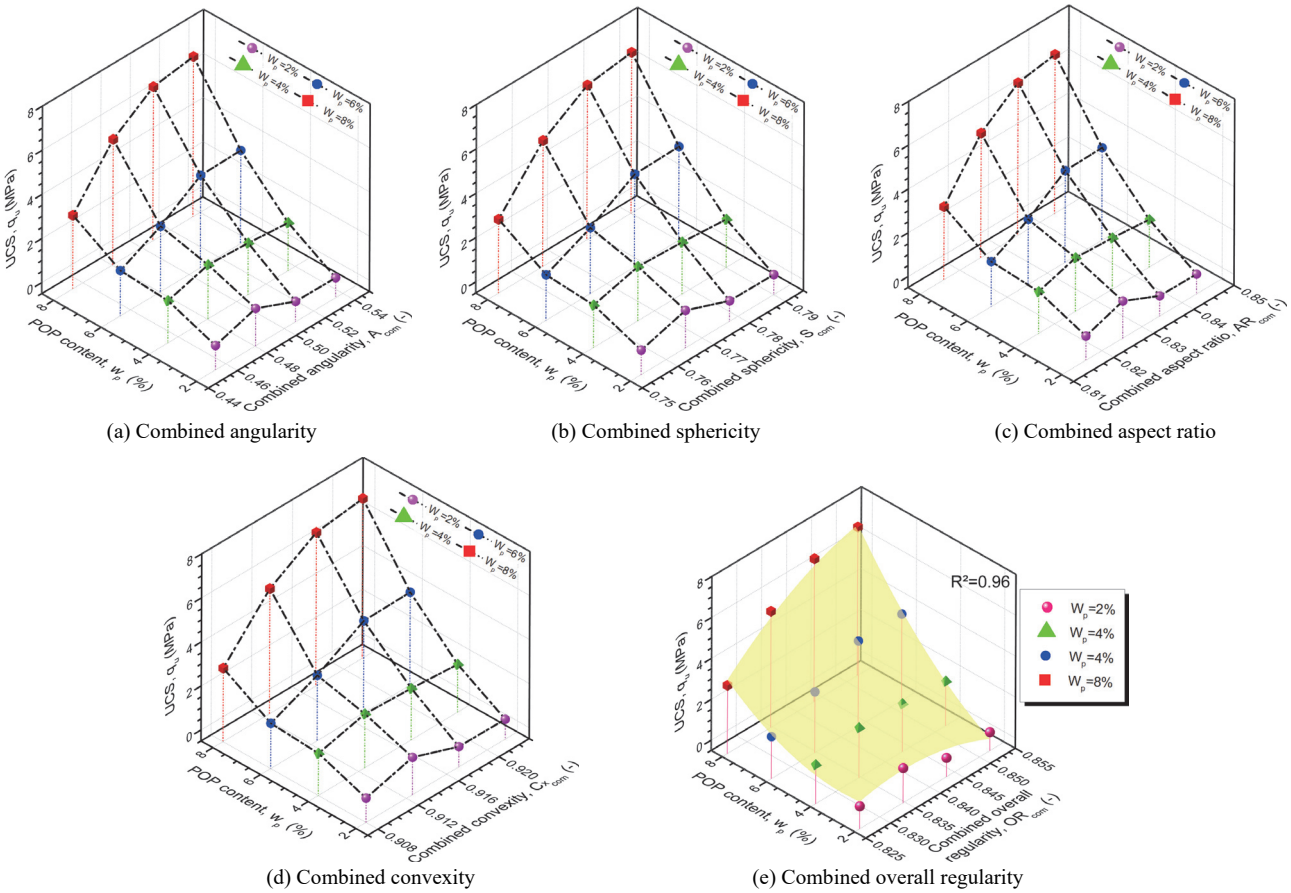

(a) Combined angularity (b) Combined sphericity (c) Combined aspect ratio

(d) Combined convexity (e) Combined overall regularity

Fig. 11 Unconfined compressive strength versus polyurethane organic polymer and particle shape properties of the tested materials

5. CORRELATION BETWEEN PARTICLE SIZE PROPERTIES AND UCS OF THE TESTED MATERIALS

In the context of assessing the unconfined compressive strength (UCS) as function of particle size properties (in terms of D_{10}, D_{50}, and C_u) and the polyurethane organic polymer percentages (W_p) of the used materials, Fig. 12 reproduces the results of the current study. As it can be observed from the 3D plot, the particle size characteristics have noticeable effects on the unconfined compressive strength of the POP-sand-fly ash mixtures, and good correlations may be expressed between these parameters with coefficient of determination (R^2 = 0.86, 0.93, and 0.94) respectively. Indeed, the decrease of effective particle diameter D_{10} and the mean particle diameter D_{50} induces a significant increasing of the unconfined compressive strength (UCS) for all used percentages of the polyurethane organic polymer (POP). Moreover, it is clearly observed that for different POP-enhanced sand-fly ash mixtures, the smaller particle sizes (D_{10} and D_{50}) exhibited higher values of the UCS of the tested materials as shown in Figs. 12(a) and 12(b). On the other hand, Fig. 12(c) presents the influence of coefficient of uniformity on the unconfined compressive strength of POP-improved sand-fly ash mixtures. It is clear from this plot that the UCS increases with the increase of the coefficient of uniformity for the different sand-fly ash mixtures under consideration. In addition, it seems from this figure that the higher coefficient of uniformity (C_u) exhibited higher values of UCS of sand-fly ash binary granular assemblies. Equations (8) to (10) are proposed to represent the variation of the unconfined compressive strength as a function of the particle size properties (D_{10}, D_{50}, and C_u) and the polyurethane organic polymer content (W_p) of the tested materials:

$$\text{UCS} = -230.37 \times (D_{10})^2 + 0.087 \times (W_p)^2 - 5.76 \times (D_{10}) \times (W_p) + 57.34 \times (D_{10}) + 0.44 \times (W_p) - 2.31 \quad (8)$$

$$\text{UCS} = -27304.9 \times (D_{50})^2 + 0.087 \times (W_p)^2 - 63.81 \times (D_{50}) \times (W_p) + 23361.7 \times (D_{50}) - 27.02 \times (W_p) - 4995.78 \quad (9)$$

$$\text{UCS} = -0.03 \times (C_u)^2 + 0.087 \times (W_p)^2 + 0.03 \times (C_u) \times (W_p) + 0.62 \times (C_u) - 0.37 \times (W_p) - 1.11 \quad (10)$$

6. PREDICTION OF UCS THROUGH THE PARTICLE CHARACTERISTICS (SHAPE AND SIZE) OF THE TESTED MATERIALS

Figures 13 to 16 illustrate comparisons between the measured test data of the tested materials and the predictions by Eqs. (7) to (10) of the unconfined compressive strength (UCS) of the POP-strengthened sand-fly ash mixtures. It is clearly observed from these figures that Eqs. (7) to (10) can much better predict the unconfined compressive strength of the sand mixed with different fly ash and polyurethane organic polymer contents. Moreover, it is found that the predicted unconfined compressive strength (UCS) values are in good agreement with the measured ones, with fitting parameters ranging from (R^2 = 0.96 to R^2 = 0.99) for the tested materials. There, it is also seen that the prediction of the POP-improved binary assemblies, shown in Fig. 13 (R^2 = 0.99), by Eq. (7) is slightly better than that by Eqs. (8) ~ (10), shown in Fig. 14 to 16 (R^2 = 0.98, 0.98, and 0.96, respectively). This again proves that the particle morphology characteristics in terms of shape and size could still be applied to evaluate and predict the unconfined compressive strength (UCS) of the polyurethane organic polymer-enhanced sand-fly ash mixtures.

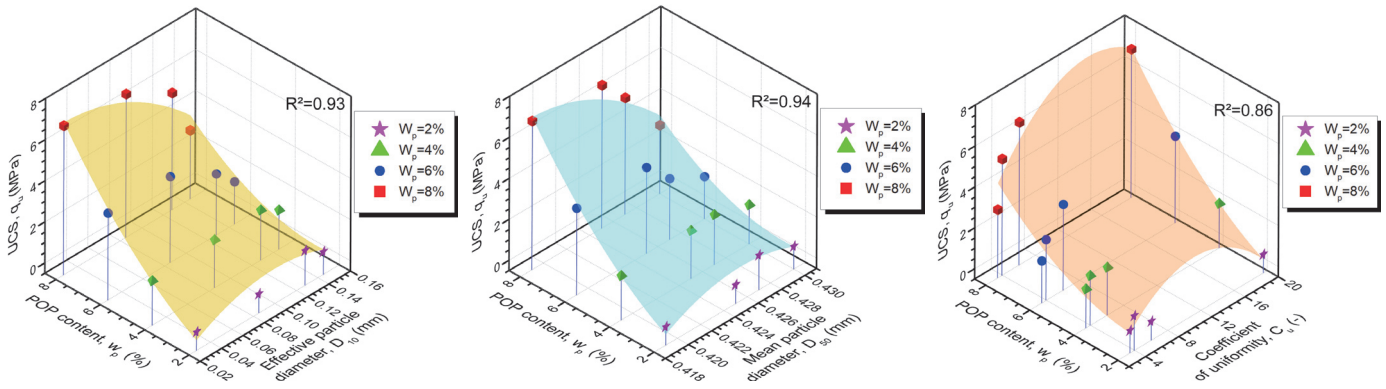

(a) Effective particle diameter (b) Mean particle diameter (c) Coefficient of uniformity

Fig. 12 Unconfined compressive strength versus polyurethane organic polymer and particle size properties of the tested materials

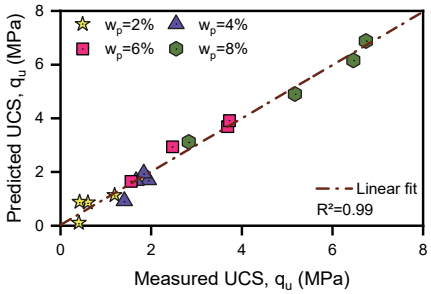

Fig. 13 Predicted UCS versus measured UCS of the tested materials using Eq. (7)

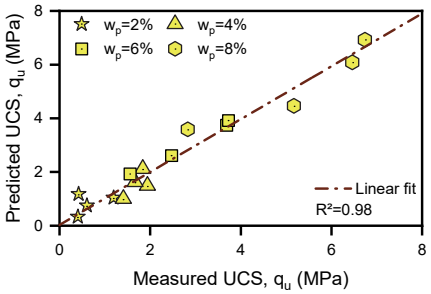

Fig. 14 Predicted UCS versus measured UCS of the tested materials using Eq. (8)

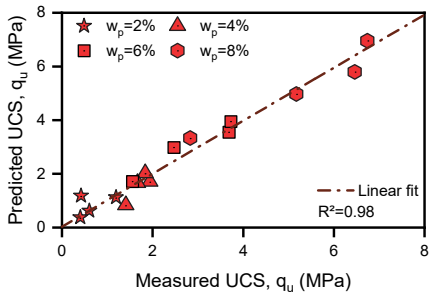

Fig. 15 Predicted UCS versus measured UCS of the tested materials using Eq. (9)

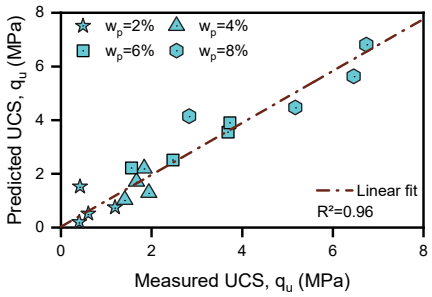

Fig. 16 Predicted UCS versus measured UCS of the tested materials using Eq. (10)

7. CONCLUSIONS

A series of unconfined compressive tests (UCT) on the POP-enhanced sand-fly ash mixture samples were carried out to elucidate the influence of the particle morphology properties (shape and size) on the UCS of the tested materials. The tested samples were mixed with the fly ash content (FA = 0%, 5%, 10%, and 15%) and polyurethane organic polymer content (W_p = 2%, 4%, 6%, and 8%). The principal findings are summarized as follows:

1. The obtained results confirm that the polyurethane organic polymer (POP) plays a major role in the enhancement of the unconfined compressive strength (UCS) of the sand-fly ash mixtures. Indeed, the uptrend is clearly observed for the polyurethane organic polymer content (W_p = 8%) and the fly ash content (FA = 15%).
2. The obtained results indicate that the particle size of the tested materials in terms of effective particle diameter D_{10}, mean particle diameter D_{50}, coefficient of uniformity C_u, and the proposed particle shape properties of sand-fly ash mixtures named as combined angularity A_{com}, combined sphericity S_{com}, combined aspect ratio AR_{com}, combined convexity Cx_{com}, combined overall regularity OR_{com} impact significantly the unconfined compressive strength of the POP-enhanced sand-fly ash mixtures. It is found that the combined overall regularity parameter (OR_{com}) appears as a reliable parameter to predict the UCS of the tested materials compared to the other particle morphology properties.
3. New developed expressions are suggested in this study to correlate the particle morphology characteristics, especially OR_{com}, D_{10}, D_{50}, and C_u with the unconfined compressive strength (UCS) of the tested sand-fly ash mixture samples improved by the polyurethane organic polymer material.

ACKNOWLEDGMENTS

This research work was carried out in the Laboratory of Materials Sciences & Environment at Hassiba Benbouali University of Chlef (Algeria). The authors are thankful to all those who effectively contributed to the achievement of this laboratory investigation.

FUNDING

The authors are grateful for the financial support received from the Directorate General for Scientific Research and Technological Development, Ministry of Higher Education and Scientific Research of Algeria.

DATA AVAILABILITY

The authors declared that all data are included in the manuscript.

CONFLICT OF INTEREST STATEMENT

The authors declare that they have no conflict of interest.

NOTATIONS

A	Area of particle (mm²)
$A+B$	Area of particle's convex hull (mm²)
A_{com}	Combined angularity
A_f	Angularity of fly ash
A_{hs}	Angularity of Host sand
AR	Aspect ratio
AR_{com}	Combined aspect ratio
AR_f	Aspect ratio of fly ash
AR_{hs}	Aspect ratio of Host sand
C_c	Coefficient of curvature
C_u	Coefficient of uniformity
Cx_{com}	Combined convexity
Cx_f	Convexity of fly ash
Cx_{hs}	Convexity of Host sand
D_{10}	Effective particle diameter (mm)
D_{50}	Mean particle diameter (mm)
DF^{min}	Minimum Feret diameter (mm)
DF^{max}	Maximum Feret diameter (mm)
D_{max}	Maximum grain size (mm)
FA	Fly ash content (%)
G_s	Specific gravity
OR	Overall regularity
OR_{com}	Combined Overall regularity
OR_f	Overall regularity of fly ash
OR_{hs}	Overall regularity of host sand
P_{eq}	Perimeter equivalent of sphere (mm)

P_r	Perimeter of the particle (mm)
POP	Polyurethane organic polymer
q_u	Axial stress at the peak stress (MPa)
R^2	Coefficient of determination
S	Sphericity
S_{com}	Combined sphericity
S_f	Sphericity of fly ash
S_{hs}	Sphericity of Host sand
SP	Poorly graded sand
UCS	Unconfined compressive strength
UCT	Unconfined compressive test
USCS	Unified soil classification system
W_p	POP content (%)
σ	Axial stress (MPa)
ε	Axial strain (%)
ε_u	Axial strain at the peak state (%)

REFERENCES

Altuhafi, F.N., Coop, M.R., and Georgiannou, V.N. (2016). "Effect of particle shape on the mechanical behavior of natural sands." *Journal of Geotechnical and Geoenvironmental Engineering*, ASCE, **142**(12), 04016071. https://doi.org/10.1061/(ASCE)GT.1943-5606.0001569

ASTM (2016). *Standard Test Method for Unconfined Compressive Strength of Cohesive Soil*. ASTM D2166/D2166M. West Conshohocken, PA.

Azaiez, H., Cherif Taiba, A., Mahmoudi, Y., and Belkhatir, M. (2021a). "Characterization of granular materials treated with fly ash for road infrastructure applications." *Transportation Infrastructure Geotechnology*, **8**, 228-253. https://doi.org/10.1007/s40515-020-00135-6

Azaiez, H., Cherif, Taiba, A., Mahmoudi, Y., and Belkhatir, M. (2021b). "Shear characteristics of fly ash improved sand as an embankment material for road infrastructure purpose." *Innovative Infrastructure Solutions*, **6**, 148. https://doi.org/10.1007/s41062-021-00517-w

Cherif Taiba, A., Mahmoudi, Y., Belkhatir, M., and Schanz, T. (2018). "Experimental investigation into the influence of roundness and sphericity on the undrained shear response of silty sand soils." *Geotechnical Testing Journal*, **41**(3). https://doi.org/10.1520/GTJ20170118

Cherif Taiba, A., Mahmoudi, Y., Hazout, L., Belkhatir, M., and Baille, W. (2019a). "Evaluation of hydraulic conductivity through particle shape and packing density characteristics of sand-silt mixtures." *Marine Georesources and Geotechnology*, **37**(10), 1175-1187. https://doi.org/10.1080/1064119X.2018.1539891

Cherif Taiba, A., Mahmoudi, Y., Hazout, L., Belkhatir, M., and Baille, W. (2019b). "Effects of gradation on the mobilized friction angle for the instability and steady states of sand-silt mixtures: Experimental evidence." *Acta Geotechnica Slovenica*, 2019/1, 79-95. https://doi.org/10.18690/actageotechslov.16.1.79-95.2019

Cherif Taiba, A., Mahmoudi, Y., Belkhatir, M., and Baille, W. (2021). "Assessment of the correlation between grain angularity parameter and friction index of sand containing low plastic fines." *Geomechanics and Geoengineering*, **16**(2), 133-149. https://doi.org/10.1080/17486025.2019.1648881

Cherif Taiba, A., Mahmoudi, Y., Azaiez, H., and Belkhatir, M. (2022). "Impact of the overall regularity and related granulometric characteristics on the critical state soil mechanics of natural sands: A state-of-the-art review." *Geomechanics and Geoengineering* (in press). https://doi.org/10.1080/17486025.2022.2044076

Cho, G.-C., Dodds, J., and Santamarina, J.C. (2006). "Particle shape effects on packing density, stiffness, and strength: Natural and crushed sands." *Journal of Geotechnical and Geoenvironmental Engineering*, ASCE, **132**(5), 591-602. https://doi.org/10.1061/(ASCE)1090-0241(2006)132:5(591)

Dai, B.B., Yang, J., and Zhou, C.Y. (2016). "Observed effects of interparticle friction and particle size on shear behavior of granular materials." *International Journal of Geomechanics*, ASCE, **16**(1), 04015011. https://doi.org/10.1061/(ASCE)GM.1943-5622.0000520

Dehghan, H., Tabarsa, A., Latifi, N., and Bagheri, Y. (2019). "Use of xanthan and guar gums in soil strengthening." *Clean Technologies and Environmental Policy*, **21**, 155-165. https://doi.org/10.1007/s10098-018-1625-0

Doumi, K., Cherif Taiba, A., Mahmoudi, Y., Belkhatir, M., and Baille, W. (2020). "Experimental investigation on the influence of relative effective diameter on ultimate shear strength of partially saturated granular soils." *Acta Geotechnica Slovenica*, 2020/1, 56-70. https://doi.org/10.18690/actageotechslov.17.1.56-70.2020

Doumi, K., Mahmoudi, Y., Cherif Taiba, A., Baille, W., and Belkhatir, M. (2021). "Infuence of the particle size on the flow potential and friction index of partially saturated sandy soils." *Transportation Infrastructure Geotechnology* (in press). https://doi.org/10.1007/s40515-021-00193-4

Frossard, E., Dano, C., Hu, W., and Hicher, P.Y. (2012). "Rockfill shear strength evaluation: A rational method based on size effects." *Geotechnique*, **62**(5), 415-427. https://doi.org/10.1680/geot.10.P.079

Ghasemzadeh, H., Modiri, F., and Darvishan, E. (2021). "A novel clean biopolymer-based additive to improve mechanical and microstructural properties of clayey soil." *Clean Technologies and Environmental Policy*, **24**, 969-981. https://doi.org/10.1007/s10098-021-02234-5

Guo, P. and Su, X. (2007). "Shear sterngth, interparticle locking, and dilatancy of granular materials." *Canadian Geotechnical Journal*, **44**(5), 579-591. https://doi.org/10.1139/t07-010

Jais, I.B.M. (2017). "Rapid remediation using polyurethane foam/resin grout in Malaysia." *Geotechnical Research*, **4**(2), 107-117. https://doi.org/10.1680/jgere.17.00003

Janalizadeh, C., Ghalandarzadeh, A., and Esmaeili, M. (2014). "Experimental study of the grading characteristic effect on liquefaction resistance of various graded sands and gravelly sands." *Arabian Journal of Geosciences*, **7**, 2739-2748. https://doi.org/10.1007/s12517-013-0886-5

Kermatikerman, M., Chegenizadeh, A., Nikraz, H., and Ayad Salih Sabbar (2017). "Experimental study on effect of fly ash on liquefaction resistance of sand." **93**, 1-6. https://doi.org/10.1016/j.soildyn.2016.11.012

Khayat, N., Ghalandarzadeh, A., and Jafari, M.K. (2014). "Grain shape effect on anisotropic behaviour of silt-sand mixtures." *Geotechnical Engineering*, **167**(3), 281-296. https://doi.org/10.1680/geng.11.00093

Kokusho, T., Hara, T., and Hiraoka, R. (2004). "Undrained shear strength of granular soils with different particle gradations." *Journal of Geotechnical and Geoenvironmental Engineering*,

130(6), 621-629. https://doi.org/10.1061/(ASCE)1090-0241(2004)130:6(621)

Ladd, R.S. (1978). "Preparing test specimens using undercompaction." *Geotechnical Testing Journal*, **1**(1), 16-23. https://doi.org/10.1520/GTJ10364J

Latifi, N., Rashid, A.S.A., Siddiqua, S., and Majid, M.Z.A. (2016). "Strength measurement and textural characteristics of tropical residual soil stabilised with liquid polymer." *Measurement*, **91**, 46-54. https://doi.org/10.1016/j.measurement.2016.05.029

Liu, J., Bai, Y., Li, D., Wang, Q., Qian, W., Wang, Y., and Wei, J. (2018). "An experimental study on the shear behaviors of polymer-sand composite materials after immersion." *Polymers*, **10**(8), 924. https://doi.org/10.3390/polym10080924

Lo, S.R. and Wardani, S.P. (2002). "Strength and dilatancy of silt stabilized by a cement and fly ash mixtures." *Canadian Geotechnical Journal*, **39**(1), 77-89. https://doi.org/10.1139/t01-062

Mahmoudi, Y., Cherif Taiba, A., Hazout, L. Belkhatir, M., and Baille, W. (2020a). "Packing density and overconsolidation ratio effects on the mechanical response of granular soils." *Geotechnical and Geological Engineering Journal*, **38**, 723-742. https://doi.org/10.1007/s10706-019-01061-2

Mahmoudi, Y., Cherif Taiba, A., Belkhatir, M., Baille, W., and Wichtmann, T. (2020b) "Characterization of mechanical behavior of binary granular assemblies through the equivalent void ratio and equivalent state parameter." *European Journal of Environmental and Civil Engineering* (in press). https://doi.org/10.1080/19648189.2020.1775708

Mahmoudi, Y., Cherif Taiba, A., Hazout, L., and Belkhatir, M. (2021). "Friction and maximum dilatancy angles of granular soils incorporating low plastic fines and depositional techniques effects." *European Journal of Environmental and Civil Engineering* (in press). https://doi.org/10.1080/19648189.2021.1999334

Mahmoudi, Y., Cherif Taiba, A., Hazout, L., and Belkhatir, M. (2022). "Comprehensive laboratory study on stress-strain of granular soils at constant global void ratio: Combined effects of fabrics and silt content." *Acta Geotechnica Slovenica* (in press). https://doi.org/10.1007/s11440-022-01480-1

Monkul, M.M., Etminan E., and Senol, A. (2016). "Infleunce of coefficient of uniformity and base sand gradation on static liquefaction of loose sand with silt." *Soil Dynamics and Earthquake Engineering*, **89**, 185-197. https://doi.org/10.1016/j.soildyn.2016.08.001

Polito, C.P. and Martin, J.R. (2001). "Effects of nonplastic fines on the liquefaction resistance of sands." *Journal of Geotechnical and Geoenvironmental Engineering*, ASCE, **127**(5), 408-415. https://doi.org/10.1061/(ASCE)1090-0241(2001)127:5(408)

Saeid, A., Amin, C., and Hamid, N. (2012). "Laboratory investigation on the compaction properties of lime and fly ash composite." *International Conference on Civil and Architectural Applications (ICCAA'2012)*, Thailand, 79-83.

Santamarina, J.C. and Cho, G.C. (2004). "Soil behaviour: The role of particle shape." in *Advances in geotechnical engineering: The Skempton Conference*, R. J. Jardine, D. M. Potts, and K. G. Higgins, Eds., 1, Thomas Telford, London, 604-617.

Su, T. and Zhang, X.C. (2011). "Effects of EN-1 soil stabilizer on slope runoff hydraulic characteristics of Pisha sandstone stabilized soil." *Transactions of the Chinese Society for Agricultural Machinery*, **42**(11), 68-75.

Tsomokos, A. and Georgiannou, V.N. (2010). "Effect of grain shape and angularity on the undrained response of fine sands." *Canadian Geotechnical Journal*, **47**(5), 539-551. https://doi.org/10.1139/T09-121

Varadarajan, A., Sharma, K.G., Venkatachalam, K., and Gupta, A.K. (2003). "Testing and modeling two rockfill materials." *Journal of Geotechnical and Geoenvironmental Engineering*, ASCE, **129**(3), 206-218. https://doi.org/10.1061/(ASCE)1090-0241(2003)129:3(206)

Wadell, H.A. (1932). "Volume, shape, and roundness of rock particles." *The Journal of Geology*, **40**(5), 443-451. https://doi.org/10.1086/623964

Wei, L.M. and Yang, J. (2014). "On the role of grain shape in static liquefaction of sand-fines mixtures." *Géotechnique*, **64**(9), 740-750. https://doi.org/10.1680/geot.14.t.013

Xiao, Y., Stuedlein, A.W., Chen, Q., Liu, H., and Liu, P. (2018). "Stress-strain strength response and ductility of gravels improved by polyurethane foam adhesive." *Journal of Geotechnical and Geoenvironmental Engineering*, ASCE, **144**(2), 04017108. https://doi.org/10.1061/(ASCE)GT.1943-5606.0001812

Xiao, Y., He, X., T. Evans, M., Stuedlein, A.W., and Liu, H. (2019). "Unconfined compressive and splitting tensile strength of basalt fiber-reinforced biocemented sand." *Journal of Geotechnical and Geoenvironmental Engineering*, ASCE, **145**(9), 04019048. https://doi.org/10.1061/(ASCE)GT.1943-5606.0002108

Yang, J. and Luo, X.D. (2015). "Exploring the relationship between critical state and particle shape for granular materials." *Journal of the Mechanics and Physics of Solids*, **84**, 196-213. https://doi.org/10.1016/j.jmps.2015.08.001

Zhang, Y.D., Buscarnera, G., and Einav, I. (2016). "Grain size dependence of yielding in granular soils interpreted using fracture mechanics, breakage mechanics and Weibull statistics." *Geotechnique*, **66**(2), 149-160. https://doi.org/10.1680/jgeot.15.P.119

Zhou, W., Yang, L., Ma, G., Chang, X., Lai, Z., and Xu, K. (2016). "DEM analysis of the size effects on the behavior of crushable granular materials." *Granular Matter*, **18**(3), 64 https://doi.org/10.1007/s10035-016-0656-7